Mechanism by which metal cofactors control substrate specificity in pyrophosphatase

Anton B. ZYRYANOV*, Alexander S. SHESTAKOV*, Reijo LAHTI† and Alexander A. BAYKOV*[1]

*A.N. Belozersky Institute of Physico-Chemical Biology and School of Chemistry, Moscow State University, Moscow 119899, Russia, and †Department of Biochemistry, University of Turku, FIN-20014 Turku, Finland

Family I soluble pyrophosphatases (PPases) exhibit appreciable ATPase activity in the presence of a number of transition metal ions, but not the physiological cofactor Mg^{2+}. The results of the present study reveal a strong correlation between the catalytic efficiency of three family I PPases (from *Saccharomyces cerevisiae*, *Escherichia coli* and rat liver) and one family II PPase (from *Streptococcus mutans*) in ATP and tripolyphosphate (P_3) hydrolysis in the presence of Mg^{2+}, Mn^{2+}, Zn^{2+} and Co^{2+} on the one hand, and the phosphate-binding affinity of the enzyme subsite P2 that interacts with the electrophilic terminal phosphate group of ATP on the other. A similar correlation was observed in *S. cerevisiae* PPase variants with modified P1 and P2 subsites. The effect of the above metal ion cofactors on ATP binding to *S. cerevisiae* PPase paralleled their effect on phosphate binding, resulting in a low affinity of Mg-PPase to ATP. We conclude that PPase mainly binds ATP and P_3 through the terminal phosphate group that is attacked by water. Moreover, this interaction is critical in creating a reactive geometry at the P2 site with these bulky substrates, which do not otherwise fit the active site perfectly. We propose further that ATP is not hydrolysed by Mg-PPase, since its interaction with the terminal phosphate is not adequately strong for proper positioning of the nucleophile–electrophile pair.

Key words: ATP, ATPase, P_i, tripolyphosphate.

INTRODUCTION

Soluble inorganic pyrophosphatase (PPase; EC 3.6.1.1) is a ubiquitous enzyme that catalyses the hydrolysis of PP_i to P_i [1]. Two non-homologous families of soluble PPase identified to date [2–4] appear to utilize similar mechanisms [5,6], presenting a remarkable example of convergent evolution of enzyme function. Metal ions are the key to catalysis by PPase. The core of the mechanism, which has been studied in detail for family I enzymes [5], is a water molecule activated for nucleophilic attack by co-ordination with two metal ions and an aspartate residue. The latter interaction is presumably a low-barrier hydrogen bond. By co-ordinating PP_i, these and one or two additional metal ions shield the negative charge on the electrophilic P_i residue and decrease the basicity of the leaving group P_i.

In the presence of its physiological activator Mg^{2+}, PPase displays nearly absolute substrate specificity. Only linear polyphosphates, such as tri- and tetra-polyphosphates, are converted besides PP_i, but at a rate that is only 1/60 of that observed with PP_i [7,8]. However, this specificity is lost when transition metal ions such as Zn^{2+}, Mn^{2+} and Co^{2+} are used as cofactors. Family I PPase displays high catalytic activity against PP_i in the presence of these metal ions, markedly increased activity against polyphosphates [7] and the ability to hydrolyse organic tri- and diphosphates, such as ATP and ADP [9,10]. ATP hydrolysis by PPase yields ADP as the primary product, which is slowly converted into AMP [7]. Catalytic activity against organic polyphosphates depends on the size of the organic moiety and varies from 1.4 % for ATP [11] to 7 % for methylpyrophosphate [12], taking activity against $MgPP_i$ as 100 %. Although the structures of several manganese and magnesium complexes of family I PPase have been solved by X-ray crystallography [5,13–15], no explanation for this change in substrate specificity is available currently.

The present study solves this long-standing puzzle by revealing a strong correlation between P_i-binding affinity and catalytic efficiency of ATP and tripolyphosphate (P_3) hydrolysis for several wild-type and variant PPases in the presence of four metal ions. The lack of catalytic activity of Mg-PPase against ATP is explained by the inability of the magnesium-bound enzyme to establish sufficiently strong interactions with the terminal phosphate that is attacked by water.

EXPERIMENTAL

Materials

Wild-type and variant yeast (*Saccharomyces cerevisiae*) cytosolic PPase (Y-PPase) [16] and wild-type *Streptococcus mutans* PPase (Sm-PPase) [17] were isolated from overproducing *Escherichia coli* XL2-Blue^b strains transformed with suitable plasmids. *E. coli* PPase (E-PPase) was isolated from the *E. coli* strain MRE-600 [18]. Rat liver cytosolic PPase (R-PPase) was obtained from rat liver [19]. All enzyme preparations were homogeneous, as verified by SDS/PAGE. The apo form of Sm-PPase was prepared and converted into Mg and Mn forms, as described previously [17]. Other PPases were preincubated for at least 1 h with the respective cations (1–2 mM). Concentrations of Y-PPase, E-PPase and Sm-PPase were calculated on the basis of their subunit molecular masses of 32.0 kDa [20], 20 kDa [18] and 33.4 kDa [17], and absorbance $A_{280}^{1\%}$ of 14.5 [21], 11.8 [8] and 3.07

Abbreviations used: K56R etc., $Lys^{56} \rightarrow Arg$ etc.; PPase, pyrophosphatase; E-PPase, PPase isolated from *Escherichia coli*; R-PPase, PPase isolated from rat liver; Sm-PPase, PPase isolated from *Streptococcus mutans*; Y-PPase, PPase isolated from *Saccharomyces cerevisiae*; P_3, tripolyphosphate; R78K, $Arg^{78} \rightarrow Lys$; Y93F, $Tyr^{93} \rightarrow Phe$.

[1] To whom correspondence should be addressed (e-mail baykov@genebee.msu.su).

[17] respectively. The concentration of R-PPase was calculated from its subunit molecular mass of 35.0 kDa [19], and the protein amounts were determined using the Bradford method [22].

Tetrasodium pyrophosphate, pentasodium P_3 and disodium ATP were obtained from Sigma. P_i and PP_i were eliminated from ATP by crystallization using water/ethanol [23].

Methods

Y-PPase and Sm-PPase activity was measured in 83 mM Tes/KOH buffer (pH 7.2), containing 17 mM KCl. Assays with Co^{2+} were performed in 100 mM Mops/KOH buffer (without KCl), since Tes binds to Co^{2+} significantly [24]. In assays with E-PPase and R-PPase, we employed 100 mM Tris/HCl buffer (without KCl). The buffers used in assays utilizing Mg^{2+} as a cofactor were supplemented with 40 μM EGTA, and BSA (0.25 mg/ml) was added to stabilize Y-PPase in assays utilizing Zn^{2+} as a cofactor. All measurements were performed at 25 °C.

ATP hydrolysis was assayed luminometrically. The assay mixture contained 0.5–1 μM ATP, metal cofactors (Mg^{2+}, Mn^{2+} or Zn^{2+}) added as chloride salts, the buffers mentioned above and various concentrations of potassium phosphate. The reaction was initiated by the addition of PPase. Aliquots (20 μl) of the assay mixture were withdrawn at 2–3 min intervals over 20–25 min and added to 0.18 ml of 0.1 M Tris/acetate buffer (pH 7.75), containing luciferase/luciferin reagent (Sigma ATP assay mix, cat. no. FL-ASC), 10 mM magnesium acetate, 2 mM EDTA, 1 mg/ml BSA and 1 mM dithiothreitol. Luminescence was measured with an LKB model 1250 luminometer. The concentration of the luciferase/luciferin reagent used was sufficient to produce a 100 mV signal for samples containing 1 μM ATP.

P_3 and PP_i hydrolysis were monitored with an automatic P_i analyser, which continuously withdraws the assay medium, mixes it with a molybdate/Methyl Green solution and measures the absorbance (A) of the resulting solution at 660 nm [25]. The sensitivity of the analyser was adjusted to 2.5–4 μM P_i/recorder scale. ATP was added to the medium as an equimolar mixture with the respective divalent cation, and the reaction was initiated by adding 0.15–10 μM P_3 or PP_i.

Alternatively, a fixed-point luminometric PP_i assay was employed to monitor PP_i hydrolysis by Sm-PPase in the presence of P_i, whereby the reaction was initiated by adding enzyme. Aliquots (192 μl) of the reaction medium were withdrawn at 15 s intervals over 1 min and incubated with 8 μl of 5 M HCl for 5 min at room temperature to inactivate PPase. The acidic solution was neutralized with 32 μl of 1.8 M Tris solution containing 16 mM $MgCl_2$ and 4.6 mM EGTA, and it was added to 18.5 μl luciferase/luciferin solution supplemented with 1.1 units/ml ATP sulphurylase (Sigma), 25 μM adenosine-5′-phosphosulphate, 13.5 mg/ml BSA and 13.5 mM dithiothreitol. ATP-sulphurylase and adenosine-5′-phosphosulphate converted residual PP_i into ATP, which was quantified from the resulting luminescence [26].

Calculations

The P_i-binding constant K_p was derived from ATP or PP_i hydrolysis curves measured in the absence or presence of added P_i by simultaneously fitting eqn. (1) with the program SCIENTIST (MicroMath), as described previously [27]. This equation, in which t is the time, [E] the free enzyme concentration and [S] the free substrate (ATP or PP_i) concentration, is a rearranged form of the Michaelis–Menten equation [28]. As [S] was quite small compared with K_m, [E] was calculated using eqn. (2), which describes complex formation between enzyme and P_i ($[E]_t$ and $[P]_t$ represent total enzyme and P_i concentrations, whereas [S] is equated to total substrate concentration) [27].

This analysis additionally yielded the ratio of the catalytic constant to the Michaelis constant (k_{cat}/K_m) for ATP hydrolysis.

$$-\frac{dS}{dt} = \frac{k_{cat}}{K_m}[E][S] \quad (1)$$

$$[E] = 0.5\left\{ [E]_t - [P]_t - K_p + \sqrt{([E]_t - [P]_t - K_p)^2 + 4K_p[E]_t} \right\} \quad (2)$$

Values of k_{cat} for PP_i were derived from the dependence of the hydrolysis rates on PP_i concentration.

Hydrolysis of P_3 to P_i proceeds through the transient formation of PP_i. As a result, catalytic and Michaelis constants derived from the dependence of actual P_i formation rate on P_3 concentration ($k_{cat,meas}$ and $K_{m,meas}$) depend on the respective parameters for P_3 and PP_i. During the steady-state phase of the reaction, the rates of P_3 hydrolysis (to yield PP_i and P_i) and PP_i hydrolysis (to yield P_i) are equivalent. Hence, the steady-state concentration of PP_i is calculated using eqn. (3), where the second part of the subscripts refers to the particular substrate. Combining eqn. (3) with rate equation (4), which describes the reaction of one enzyme with two substrates (v is the rate and $[E]_0$ the total enzyme concentration), a simple Michaelis–Menten equation is obtained with parameters specified by eqns. (5) and (6). These equations were used to estimate true k_{cat,P_3} and K_{m,P_3} values from $k_{cat,meas}$ and $K_{m,meas}$ and the known $k_{cat,PP}$ value.

$$\frac{k_{cat,PP}}{K_{m,PP}}[PP_i] = \frac{k_{cat,P_3}}{K_{m,P_3}}[P_3] \quad (3)$$

$$\frac{v}{[E]_0} = \frac{k_{cat,P_3}}{1 + K_{m,P_3}(1 + [PP_i]/K_{m,PP})/[P_3]} + \frac{k_{cat,PP}}{1 + K_{m,PP}(1 + [P_3]/K_{m,P_3})/[PP_i]} \quad (4)$$

$$k_{cat,meas} = \frac{k_{cat,P_3}k_{cat,PP}}{k_{cat,P_3} + k_{cat,PP}} \quad (5)$$

$$K_{m,meas} = \frac{K_{m,P_3}k_{cat,PP}}{k_{cat,P_3} + k_{cat,PP}} \quad (6)$$

The K_m values for ATP were derived from ATP inhibition of P_3 hydrolysis. In these experiments, ATP acted as a competing substrate that was slowly converted and its effect analysed using an equation analogous to eqn. (4). As the k_{cat}/K_m value for ATP was determined separately, this analysis also yielded k_{cat} for ATP hydrolysis.

RESULTS

Catalytic efficiency of Y-PPase in the presence of various metal ions

Michaelis–Menten parameters were determined for three substrates (ATP, P_3 and PP_i) in the presence of four metal ions (Mg^{2+}, Mn^{2+}, Zn^{2+} and Co^{2+}) (Table 1). For both ATP and P_3, k_{cat}/K_m was much lower for Mg^{2+} than for other metal cofactors. This parameter represents the enzyme preference for a given substrate because when several substrates are available to enzyme, their rates of consumption are proportional to the respective k_{cat}/K_m values [eqn. (1)].

In agreement with previous reports [7,9,10], k_{cat} values were comparable for the three substrates in the presence of Mn^{2+}, Zn^{2+} and Co^{2+} as cofactors. With Mg^{2+}, k_{cat} increased markedly for

Table 1 Parameters for ATP, P_3 and PP_i hydrolysis and phosphate binding by Y-PPase in the presence of different metal cofactors

Metal cofactor	Concentration (mM)	k_{cat}/K_m ($mM^{-1} \cdot s^{-1}$)		K_m (μM)		k_{cat} (s^{-1})			
		ATP	P_3	ATP	P_3	ATP	P_3	PP_i	K_p (μM)
Mg^{2+}	5	< 0.001	2.0 ± 0.2	4800 ± 800* (4900 ± 400)†	24 ± 2	< 0.005	0.049	260	1000‡
Mn^{2+}	1	12 ± 1	6300 ± 500	150 ± 30*	0.4 ± 0.3	1.8	2.3	7.6	0.51 ± 0.04
Zn^{2+}	1	62 ± 3	$11\,000 \pm 1000$	40 ± 10*	2.0 ± 0.1	2.7	21	24	2.7 ± 0.3
Co^{2+}	0.5	1.3 ± 0.1	800 ± 100	80 ± 10*	2.6 ± 0.3	0.10	2.1	2.5	13 ± 1

* Calculated from ATP inhibition of P_3 hydrolysis (Figure 2).
† Calculated from ATP inhibition of PP_i hydrolysis.
‡ Calculated from P_i concentration dependence of enzyme-bound PP_i formation [29].

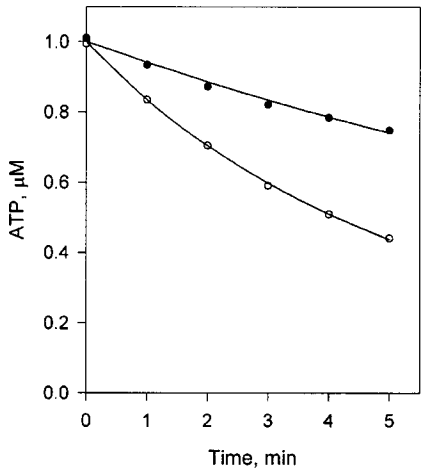

Figure 1 Effect of P_i on ATP hydrolysis by 50 nM Y-PPase in the presence of 1 mM Zn^{2+}

The initial concentration of ATP was 1 μM. ○, no P_i added; ●, 5 μM P_i. The lines show the best fit to eqns. (1) and (2) with parameters given in Table 1.

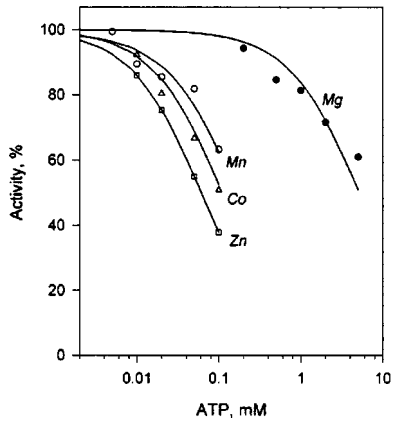

Figure 2 ATP inhibition of P_3 hydrolysis catalysed by Y-PPase in the presence of different metal cofactors (indicated by curve labels)

The specific-activity values shown correspond to P_i production rates measured in the presence of both P_3 and ATP minus the rates measured with ATP only. Specific activity measured without ATP was taken as 100% in each case, and the actual values were 0.0145 s^{-1} (Mg^{2+}), 0.59 s^{-1} (Mn^{2+}), 3.7 s^{-1} (Zn^{2+}) and 0.30 s^{-1} (Co^{2+}). The initial concentration of P_3 was 10 μM (Mg^{2+}), 0.15 μM (Mn^{2+}), 0.5 μM (Zn^{2+}) or 0.5 μM (Co^{2+}), and the concentrations of the metal cofactors were as given in Table 1.

PP_i and decreased for P_3 and, in particular, for ATP, with which no activity was detected.

P_i and ATP-binding affinities of Y-PPase in the presence of various metal ions

The dissociation constant K_p, characterizing PPase affinity for the reaction product (phosphate), was estimated from P_i inhibition of ATP hydrolysis. At ATP concentrations much lower than K_m, practically all the enzyme is present in the free form in the absence of P_i, and the effect of P_i on ATP hydrolysis rate is a direct measure of P_i binding. This method was described in detail in a recent paper [27]. Figure 1 shows representative data for Zn-PPase. The value of K_p for Mg-PPase (which does not support ATPase activity) was obtained from an earlier investigation [29] on P_i concentration dependence of enzyme-bound PP_i formation at equilibrium with P_i in the medium. The K_p values listed in Table 1 indicate weak P_i binding in the presence of Mg^{2+} and tight binding in the presence of transition metal cofactors. In all cases, the K_p value represents the first P_i molecule that binds to the enzyme (the PPase active site can accommodate two P_i molecules).

ATP binding to Y-PPase was characterized by the Michaelis constant K_m, estimated from inhibition of P_3 hydrolysis (Figure 2). In these experiments, ATP was an alternative substrate that was slowly converted. For the interpretation of the K_m values, it is important to note that the time course of Co^{2+}-supported ATP hydrolysis exhibited no lag or burst during the pre-steady-state phase (results not shown), indicating that the rate-determining step of this reaction is the P–O bond breakdown. In this case, the K_m value sets the upper limit for the dissociation constant of enzyme–ATP complex. In the presence of Mg^{2+}, ATP was not hydrolysed and thus acted as a true competitive inhibitor. As specified in Table 1, K_m values were much higher for Mg^{2+} than the other metal-ion cofactors tested.

Table 1 also lists true K_m values for P_3 calculated using eqn (6). At least with the Mg^{2+} cofactor, the K_m value measures the true dissociation constant for the enzyme–substrate complex, keeping in mind the low k_{cat} value (see the Discussion section for details).

ATP hydrolysis and P_i binding by different PPases

Table 2 presents k_{cat}/K_m values for ATP hydrolysis and K_p values for two other family I PPases (from *E. coli* and rat liver) and one family II PPase (from *S. mutans*). With Sm-PPase, which displays no ATPase activity (Table 2), K_p was calculated by examining the

Table 2 Parameters for ATP hydrolysis and phosphate binding by different PPases in the presence of Mg^{2+} and Mn^{2+}

Metal ion concentrations used: E-PPase, 1 mM Mg^{2+} and Mn^{2+}; R-PPase, 1 mM Mg^{2+} and 0.6 mM Mn^{2+}; Sm-PPase, 5 mM Mg^{2+} and 0.5 mM Mn^{2+}.

	Mn^{2+}		Mg^{2+}	
Enzyme	k_{cat}/K_m ($mM^{-1} \cdot s^{-1}$)	K_p (μM)	k_{cat}/K_m ($mM^{-1} \cdot s^{-1}$)	K_p (μM)
E-PPase	8 ± 1	0.63 ± 0.08*	< 0.3	850–1550†‡
R-PPase	4.2 ± 0.4	0.7 ± 0.2*	< 0.1	2600 ± 600†§
Sm-PPase	< 0.01	> 2000‖	< 0.01	2500‖

* Calculated from P_i inhibition of ATP hydrolysis.
† Calculated from P_i concentration dependence of enzyme-bound PP_i formation.
‡ From Käpylä et al. [30].
§ From Smirnova et al. [31].
‖ Calculated from P_i inhibition of PP_i hydrolysis (Figure 3).

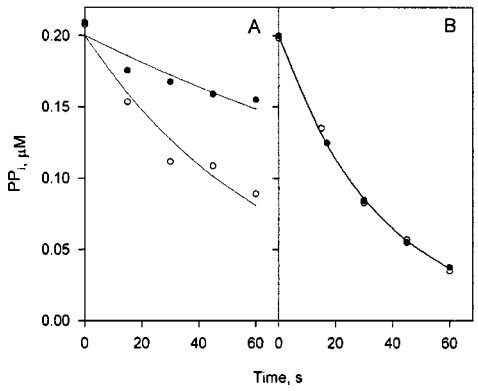

Figure 3 Effect of P_i on PP_i hydrolysis by 0.3 nM Sm-PPase in the presence of 5 mM Mg^{2+} (A) and 0.7 nM Sm-PPase in the presence of 0.5 mM Mn^{2+} (B)

PP_i hydrolysis was performed, followed by the luminometric procedure. The initial concentration of PP_i was 0.2 μM. ○, no P_i added; ●, 5 mM P_i (**A**) or 0.5 mM P_i (**B**). The lines show the best fit to eqns. (1) and (2) with parameters given in Table 2.

Table 3 Parameters for ATP hydrolysis and phosphate binding by Y-PPase variants in the presence of 1 mM Mn^{2+}

Variant	k_{cat}/K_m ($mM^{-1} \cdot s^{-1}$)	K_p (μM)
K56R	0.26 ± 0.01	14 ± 1
R78K	48 ± 1	1.6 ± 0.1
Y93F	0.39 ± 0.01	190 ± 30
K193R	4.2 ± 0.2	1.4 ± 0.1

effect of P_i on PP_i hydrolysis (Figure 3). Both family I enzymes exhibited measurable ATPase activity and high P_i-binding affinity in the presence of Mn^{2+}, but not Mg^{2+}. In contrast, Sm-PPase was ineffective in ATP hydrolysis and bound P_i weakly in the presence of either Mg^{2+} or Mn^{2+}.

Hydrolysis of 5 μM PP_i, catalysed by Sm-PPase in the presence of 0.5 mM Mn^{2+}, was not inhibited by 100 μM ATP (results not shown). The Michaelis constant for this enzyme in the presence of Mn^{2+} was estimated as 96 μM [17], setting the lower limit for the ATP-binding constant at 1 mM.

Effects of active-site substitutions on ATP hydrolysis and P_i binding by Y-PPase

Lys^{56} and Tyr^{93} residues of the protein specifically bind the electrophilic phosphate group of PP_i (i.e. the group attacked by water), whereas Arg^{78} and Lys^{193} residues interact with the leaving group phosphate in Y-PPase [5]. $Lys^{56} \rightarrow$ Arg (K56R) and $Tyr^{93} \rightarrow$ Phe (Y93F) substitutions decreased the k_{cat}/K_m value measured in the presence of Mn^{2+} by 27- and 370-fold respectively, whereas the effects of two other substitutions [$Arg^{78} \rightarrow$ Lys (R78K) and K193R] were much less marked, and the effect was reversed in the case of R78K (3-fold increase) (Table 3; for wild-type Y-PPase, see Table 1). The effects of the substitutions on P_i binding were similar in that K_p was only slightly increased in R78K and K193R variants (to 1.6 and 1.4 μM) when compared with the wild-type enzyme (0.51 μM), but drastically increased (to 14 and 190 μM) in K56R and Y93F variants (Tables 1 and 3).

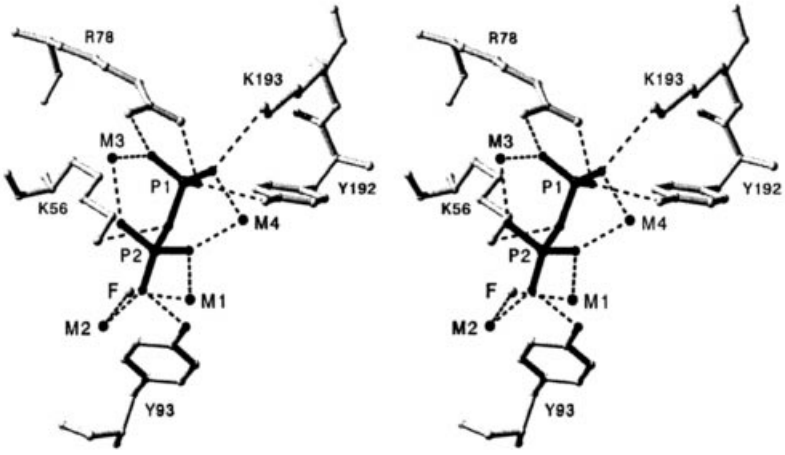

Figure 4 Structure of the Y-PPase active site containing bound PP_i [5]

Pyrophosphate (P1–P2) and metal ions (M1–M4) are shown in black. The grey circle (F) is a fluoride ion replacing nucleophilic water/hydroxide. Hydrogen bonds and electrostatic interactions are represented by broken lines. The Figure was created using Swiss-PdbViewer [34].

DISCUSSION

Family I PPases appear to use Mg^{2+} as cofactor in *in vivo* PP_i hydrolysis, whereas family II PPases may use both Mg^{2+} and Mn^{2+}, as bacteria possessing family II enzymes accumulate large amounts of both cations [32,33]. Therefore the inability of the respective physiological cofactors to support the ATPase activity of these enzymes has a clear physiological significance, since it prevents futile ATP hydrolysis. In contrast, non-physiological cofactors, such as Mn^{2+}, Zn^{2+} and Co^{2+}, support both PPase [21] and ATPase activities [9,10] in family I enzymes. The results of the present study, together with those of the structural studies on Y-PPase, provide an explanation for this interesting phenomenon.

X-ray crystallographic analyses have led to the identification of two phosphate-binding subsites, P1 and P2, within the active sites of PPases of both families [5,6]. In Y-PPase, P1 is formed by Arg^{78}, Tyr^{192}, Lys^{193} and metal ions M3–M4, whereas P2 constitutes interactions between Lys^{56}, Tyr^{93} and metal ions M1–M4 (Figure 4). This active-site structure is completely conserved in other PPases of family I, including E-PPase [2,14], and to a large extent, in Sm-PPase belonging to family II [6]. The contributions of P1 and P2 to the PP_i-binding affinity of Y-PPase are similar in the presence of Mg^{2+}, as revealed by comparable binding constants for the two P_i molecules [29,35]. In contrast, P_i binding to one of the subsites is dramatically enhanced (four or five orders of magnitude) in the presence of transition metal ions, such as Mn^{2+} and Co^{2+} [36]. Recent studies [27] have identified this subsite as P2, where phosphate interacts with all four metal ions in the PPase active site (Figure 4). Of the two phosphate groups accommodated within the PPase active site, the terminal group occupying P2 appears to participate in the more important interactions, which not only position the electrophilic phosphorus atom and compensate the negative charges of its oxygen partners, but also generate nucleophilic water/hydroxide by positioning M1 and M2 closer to each other. As a result, one of the two water molecules bridging M1 and M2 in the 'resting' enzyme [37] is expelled, thereby generating a strongly nucleophilic water molecule simultaneously linked to M1 and M2 [5,37].

Another inference from structural studies is that the PPase active site is preformed to bind PP_i. Of 18 lone electron pairs of PP_i, 15 are co-ordinated to enzyme groups, either directly or through metal ions in the enzyme–substrate complex stabilized by fluoride [5]. Attempts to model the three-dimensional structure of Y-PPase–ATP complex (N.A. Kisseleva and A.A. Baykov, unpublished work) revealed fewer stabilizing interactions and that significant distortion of the active site is required to accommodate the bulky ATP molecule. Hence, the k_{cat}/K_m value increases upon replacement of Arg^{78} with the smaller lysine residue at P1 (Tables 1 and 3). This is consistent with the view that PP_i and organic substrates are bound by PPase in somewhat different modes [38].

The results shown in Tables 1–3 indicate a correlation between the catalytic efficiency of PPase in ATP and P_3 hydrolysis and substrate-binding affinity (as characterized by K_m) and P_i-binding affinity of the subsite P2. This correlation extends to four different PPases belonging to two families, four metal cofactors and two substrates. In all instances, K_p and K_m values are high in the presence of Mg^{2+} and absence of ATPase, and low tripolyphosphatase activity is observed. In contrast, low K_p values for Mn^{2+}, Zn^{2+} or Co^{2+} correspond to low K_m values and significant ATPase activity. The behaviour of Sm-PPase is particularly interesting, since this enzyme displays very high K_p in the presence of both Mg^{2+} and Mn^{2+} and possesses no ATPase activity with either cofactor. Moreover, mutations that significantly increase K_p (K56R and Y93F) strongly inhibit the ATPase activity of Y-PPase. Importantly, both these mutations are located at subsite P2.

These results can be explained by assuming that stronger binding of the terminal phosphate group of bulky substrates in the presence of transition metal ions allows more favourable positioning for catalysis. In the presence of transition metal ions, ATP and P_3 binding is dominated by interactions at P2, and significantly (but not precisely) resembles PP_i binding as indicated by a comparison of k_{cat} values. Although similar steric constraints from the ADP moiety of ATP are expected in the presence of Mg^{2+}, they are not counterbalanced by a strong interaction at the P2 site, resulting in improper positioning of the terminal phosphate group with respect to M1 and M2 (Figure 4) and, presumably, inability to generate the bridging water nucleophile. A similar mispositioning is expected for P_3, which is hydrolysed slowly by the Mg-bound enzyme (Table 1).

This explanation implies that low efficiency of Mg-PPase in catalysis of ATP and P_3 hydrolysis is due to low rate of P–O bond breakage in these substrates and that transition metal ions accelerate this step. Indeed, the rate constants for product (P_i and PP_i) release from Y-PPase in the presence of Mg^{2+} (800 and 33 s^{-1} respectively; [39]) exceed k_{cat} for P_3 hydrolysis (0.049 s^{-1}; Table 1) by many orders of magnitude. On the other hand, recent pre-steady-state kinetic studies on Y-PPase catalysis of PP_i hydrolysis indicated that release of the second P_i product is slowed down and becomes the rate-determining step in the presence of transition metal ions (P. Halonen, A. A. Baykov, A. Goldman, R. Lahti and B. S. Cooperman, unpublished work). The similarity of the k_{cat} values for P_3 and PP_i in the presence of Zn^{2+} or Co^{2+} (Table 1) indicates that P_i release is also the slowest step in P_3 hydrolysis. Thus transition metal ions appear to have two opposite effects on PPase: they accelerate P–O bond cleavage in ATP and P_3 but they decelerate P_i release compared with Mg^{2+}. The former effect is smaller for ATP than for P_3, implying that the P–O bond breakage is the rate-determining step in ATP hydrolysis, as also indicated by the pre-steady-state results on Co^{2+}-supported ATP hydrolysis mentioned above and by the observation that the k_{cat} value is lower for ATP than for PP_i in the presence of transition metal ions (Table 1).

Vainonen et al. [38] recently suggested that the higher efficiency of transition metal ions in PPase-catalysed ATP hydrolysis, compared with that of Mg^{2+}, results from a greater polarizing effect on nucleophilic water. However, in the framework of this hypothesis, it is hard to explain why Mn^{2+} does not confer ATPase activity to Sm-PPase (Table 2), despite being more effective than Mg^{2+} in PP_i hydrolysis [17].

An issue that remains to be elucidated is why the binding capacity of P2 is so weak in family II PPases and is dependent on the nature of the metal cofactor in family I PPases. In solution, P_i forms complexes of similar stability with all the metal ions used in the present study. Analyses of the effects of metal ions on the structures of P_i complexes of PPase should clarify this issue. However, no such structures are currently available for Mg-PPase of either family. Interestingly, although Mg^{2+} alone is ineffective as a cofactor in ATP hydrolysis, this metal ion significantly stimulates the Mn^{2+}-supported reaction catalysed by yeast PPase [10]. This implies that only some of the four metal ions bound within the enzyme–substrate complex (Figure 4) are critical in determining substrate specificity. An exchange-inert $Co(NH_3)_3(P_3)$ complex is hydrolysed by yeast PPase in the presence of Zn^{2+} but not Mg^{2+} [40], suggesting that substrate specificity is determined by the metal ions bound to protein (M1–M2) rather than the substrate.

None of the specific Mg^{2+}-dependent ATPases, including F_1-ATPase and myosin ATPase, appear to utilize the 3/4-metal

mechanism of catalysis that is efficiently employed by PPases (1). The low efficiency of this mechanism in ATP hydrolysis may be explained as follows: upon breakage of the P–O bond, the distance between the β- and γ-P atoms increases. In PPase, this is achieved by the movement of the leaving group phosphate, allowing the organization of a highly efficient but inevitably rigid nucleophilic centre cross-linked with metal ions (Figure 4). In specific ATPases, the leaving group, ADP, is fairly bulky and participates in many interactions, thus providing the required nucleotide specificity. It is, therefore, both structurally and energetically more favourable to move the electrophilic group phosphate than the leaving group ADP in ATPases. As a consequence of its flexibility, the nucleophilic centre is less efficient in ATPases and the catalytic constant never reaches 10^4 s^{-1}, which is observed for family II PPases.

This work was supported by grants from the Russian Foundation for Basic Research (grant nos. 00-04-48310, 00-15-97907 and 01-04-06113) and the Finnish Academy of Sciences (grant nos. 35736 and 47513).

REFERENCES

1 Baykov, A. A., Cooperman, B. S., Goldman, A. and Lahti, R. (1999) Cytoplasmic inorganic pyrophosphatase. Progr. Mol. Subcell. Biol. **23**, 127–150

2 Sivula, T., Salminen, A., Parfenyev, A. N., Pohjanjoki, P., Goldman, A., Cooperman, B. S., Baykov, A. A. and Lahti, R. (1999) Evolutionary aspects of inorganic pyrophosphatase. FEBS Lett. **454**, 75–80

3 Young, T. W., Kuhn, N. J., Wadeson, A., Ward, S., Burges, D. and Cooke, G. D. (1998) *Bacillus subtilis* ORF yybQ encodes a manganese-dependent inorganic pyrophosphatase with distinctive properties: the first of a new class of soluble pyrophosphatase? Microbiology **144**, 2563–2571

4 Shintani, T., Uchiumi, T., Yonezawa, T., Salminen, A., Baykov, A. A., Lahti, R. and Hachimori, A. (1998) Cloning and expression of a unique inorganic pyrophosphatase from *Bacillus subtilis*: evidence for a new family of enzymes. FEBS Lett. **439**, 263–266

5 Heikinheimo, P., Tuominen, V., Ahonen, A.-K., Teplyakov, A., Cooperman, B. S., Baykov, A. A., Lahti, R. and Goldman, A. (2001) Toward a quantum-mechanical description of metal-assisted phosphoryl transfer in pyrophosphatase. Proc. Natl. Acad. Sci. U.S.A. **98**, 3121–3126

6 Merckel, M. C., Fabrichniy, I. P., Salminen, A., Kalkkinen, N., Baykov, A. A., Lahti, R. and Goldman, A. (2001) Crystal structure of *Streptococcus mutans* pyrophosphatase: a new fold for an old mechanism. Structure (London) **9**, 289–297

7 Höhne, W. E. and Heitmann, P. (1974) Tripolyphosphate as a substrate of the inorganic pyrophosphatase from baker's yeast; the role of divalent metal ions. Acta Biol. Med. Germ. **33**, 1–14

8 Josse, J. (1966) Constitutive inorganic pyrophosphatase of *Escherichia coli.* 1. Purification and catalytic properties. J. Biol. Chem. **231**, 1938–1947

9 Schlesinger, M. J. and Coon, M. J. (1960) Hydrolysis of nucleoside di- and triphosphates by crystalline preparations of yeast inorganic pyrophosphatase. Biochim. Biophys. Acta **41**, 30–36

10 Kunitz, M. (1961) Hydrolysis of adenosine triphosphate by crystalline yeast pyrophosphatase. J. Gen. Physiol. **45**, 31–46

11 Baykov, A. A. and Avaeva, S. M. (1974) Regulation of yeast inorganic-pyrophosphatase activity by divalent cations. Eur. J. Biochem. **47**, 57–66

12 Mel'nik, M. S., Nazarova, T. I. and Avaeva, S. M. (1982) Methylpyrophosphate, the simplest organic substrate of yeast inorganic pyrophosphatase. Biokhimiya **47**, 323–328

13 Kankare, J., Salminen, T., Lahti, R., Cooperman, B., Baykov, A. A. and Goldman, A. (1996) Crystallographic identification of metal-binding sites in *Escherichia coli* inorganic pyrophosphatase. Biochemistry **35**, 4670–4677

14 Harutyunyan, E. H., Oganessyan, V. Yu., Oganessyan, N. N., Avaeva, S. M., Nazarova, T. I., Vorobyeva, N. N., Kurilova, S. A., Huber, R. and Mather, T. (1997) Crystal structure of holo inorganic pyrophosphatase from *Escherichia coli* at 1.9 Å resolution. Mechanism of hydrolysis. Biochemistry **36**, 7754–7760

15 Harutyunyan, E. H., Oganessyan, V. Yu., Oganessyan, N. N., Terzyan, S. S., Popov, A. N., Rubinskiy, S. B., Vainstein, B. K., Nazarova, T. I., Kurilova, S. A., Vorobyeva, N. N. et al. (1996) The structure of *Escherichia coli* inorganic pyrophosphatase and its complex with Mn^{2+} ion at 2.2 Å resolution. Kristallografiya **41**, 84–96

16 Heikinheimo, P., Pohjanjoki, P., Helminen, A., Tasanen, M., Cooperman, B. S., Goldman, A., Baykov, A. and Lahti, R. (1996) A site-directed mutagenesis study of *Saccharomyces cerevisiae* pyrophosphatase. Functional conservation of the active site of soluble inorganic pyrophosphatases. Eur. J. Biochem. **239**, 138–143

17 Parfenyev, A. N., Salminen, A., Halonen, P., Hachimori, A., Baykov, A. A. and Lahti, R. (2001) Quaternary structure and metal ion requirement of family II pyrophosphatases from *Bacillus subtilis*, *Streptococcus gordonii*, and *Streptococcus mutans*. J. Biol. Chem. **276**, 24511–24518

18 Wang, S. C. K., Hall, D. C. and Josse, J. (1970) Constitutive inorganic pyrophosphatase of *Escherichia coli*. 3. Molecular weight and physical properties of the enzyme and its subunits. J. Biol. Chem. **245**, 4335–4345

19 Smirnova, I. N., Kudryavtseva, N. A., Komissarenko, S. V., Tarusova, N. B. and Baykov, A. A. (1988) Diphosphonates are potent inhibitors of mammalian inorganic pyrophosphatase. Arch. Biochem. Biophys. **267**, 280–284

20 Kolakowski, Jr, L. F., Schloesser, M. and Cooperman, B. S. (1988) Cloning, molecular characterization and chromosomal localization of the inorganic pyrophosphatase (*PPA*) gene from *S. cerevisiae*. Nucleic Acids Res. **16**, 10441–10452

21 Kunitz, M. (1952) Crystalline inorganic pyrophosphatase isolated from baker's yeast. J. Gen. Physiol. **35**, 423–450

22 Bradford, M. M. (1976) A rapid and sensitive method for the quantitation of microgram quantities of protein utilizing the principle of protein–dye binding. Anal. Biochem. **72**, 248–254

23 Berger, L. (1956) Crystallization of the sodium salt of adenosine triphosphate. Biochim. Biophys. Acta **20**, 23–26

24 Vanni, A. and Gastaldi, D. (1986) The interaction of bivalent metal ions (Zn^{2+}, Cu^{2+}, Co^{2+}, Ni^{2+}) with TES. Annali de Chimica (Rome) **76**, 375–385

25 Baykov, A. A. and Avaeva, S. M. (1981) A simple and sensitive apparatus for continuous monitoring of orthophosphate in the presence of acid-labile compounds. Anal. Biochem. **116**, 1–4

26 Nyrén, P. and Lundin, A. (1985) Enzymatic method for continuous monitoring of inorganic pyrophosphate synthesis. Anal. Biochem. **151**, 504–509

27 Zyryanov, A. B., Pohjanjoki, P., Kasho, V. N., Shestakov, A. S., Goldman, A., Lahti, R. and Baykov, A. A. (2001) The electrophilic and leaving group phosphates in the catalytic mechanism of yeast pyrophosphatase. J. Biol. Chem. **276**, 17629–17634

28 Fersht, A. (1999) Structure and Mechanism. In Protein Science, pp. 116–117, W.H. Freeman and Company, New York

29 Baykov, A. A. and Shestakov, A. S. (1992) Two pathways of pyrophosphate hydrolysis and synthesis by yeast inorganic pyrophosphatase. Eur. J. Biochem. **206**, 463–470

30 Käpylä, J., Hyytiä, T., Lahti, R., Goldman, A., Baykov, A. A. and Cooperman, B. S. (1995) Effect of D97E substitution on the kinetic and thermodynamic properties of *Escherichia coli* inorganic pyrophosphatase. Biochemistry **34**, 792–800

31 Smirnova, I. N., Kasho, V. N., Volk, S. E., Ivanov, A. H. and Baykov, A. A. (1995) Rates of elementary steps catalysed by rat liver cytosolic and mitochondrial inorganic pyrophosphatases in both directions. Arch. Biochem. Biophys. **318**, 340–348

32 Charney, J., Fisher, W. P. and Hegarty, C. P. (1951) Manganese as an essential element for sporulation in the genus *Bacillus*. J. Bacteriol. **62**, 145–148

33 Martin, M. E., Byers, B. R., Olson, M. O. J., Salin, M. L., Arceneaux, J. E. L. and Tolbert, C. (1986) A *Streptococcus mutans* superoxide dismutase that is active with either manganese or iron as a cofactor. J. Biol. Chem. **261**, 9361–9367

34 Guex, N. and Peitsch, M. C. (1997) SWISS-MODEL and the Swiss-PdbViewer: an environment for comparative protein modeling. Electrophoresis **18**, 2714–2723

35 Springs, B., Welsh, K. M. and Cooperman, B. S. (1981) Thermodynamics, kinetics, and mechanism in yeast inorganic pyrophosphatase catalysis of inorganic pyrophosphate: inorganic phosphate equilibration. Biochemistry **20**, 6384–6391

36 Cooperman, B. S., Panackal, A., Springs, B. and Hamm, D. J. (1981) Divalent metal ion, inorganic phosphate, and inorganic phosphate analogue binding to yeast inorganic pyrophosphatase. Biochemistry **20**, 6051–6060

37 Heikinheimo, P., Lehtonen, J., Baykov, A., Lahti, R., Cooperman, B. and Goldman, A. (1996) The structural basis for pyrophosphatase catalysis. Structure (London) **4**, 1491–1508

38 Vainonen, Yu. P., Rodina, E. V., Vorobyeva, N. N., Kurilova, S. A., Nazarova, T. I. and Avaeva, S. M. (2001) Characterstics of organic and inorganic substrate hydrolysis by *Escherichia coli* inorganic pyrophosphatase in the presence of different metal ion activators. Izv. Akad. Nauk **10**, 1793–1799

39 Baykov, A. A., Fabrichniy, I. P., Pohjanjoki, P., Zyryanov, A. B. and Lahti, R. (2000) Fluoride effects along the reaction pathway of pyrophosphatase. Evidence for a second enzyme · pyrophosphate intermediate. Biochemistry **39**, 11939–11947

40 Knight, W. B., Ting, S.-J., Chuang, S., Dunaway-Mariano, D., Haromy, T. and Sundaralingam, M. (1983) Yeast inorganic pyrophosphatase substrate recognition. Arch. Biochem. Biophys. **227**, 302–309

Received 6 June 2002/19 July 2002; accepted 9 August 2002
Published as BJ Immediate Publication 9 August 2002, DOI 10.1042/BJ20020880